Hindawi
Wireless Communications and Mobile Computing
Volume 2021, Article ID 5573946, 14 pages
https://doi.org/10.1155/2021/5573946

Research Article

Performance of Optical Mobile Communications with User Mobility and Multiple Light Sources

Jian Dang,[1,2] **Jiajun Gao**,[1] **Zaichen Zhang**,[1,2] **Liang Wu**,[1,2] **Bingcheng Zhu**,[1] **Chunguo Li**,[3] **and Jiangzhou Wang**[4]

[1]*National Mobile Communications Research Laboratory, Southeast University, Nanjing 210096, China*
[2]*Purple Mountain Laboratory, Nanjing 211111, China*
[3]*School of Information Science and Engineering, Southeast University, Nanjing 210096, China*
[4]*School of Engineering and Digital Arts, University of Kent, Canterbury CT2 7NT, UK*

Correspondence should be addressed to Zaichen Zhang; zczhang@seu.edu.cn

Received 11 February 2021; Revised 24 June 2021; Accepted 24 August 2021; Published 14 September 2021

Academic Editor: Alessandro Bazzi

Optical mobile communication (OMC) is a recently proposed optical wireless communication concept aiming to provide very high-speed data rate optical wireless links for multiple and, in general, distributed mobile users. Previous work analyzed the rate performance of a two-user OMC system without user mobility. This paper extends the rate analysis to multiple users with mobility. The scenario of employing multiple light sources with possible user grouping is also considered. User mobility and multiple light sources lead to new challenges on the system design which are addressed for broadcast downlink communication in this work. Simulations show that user mobility decreases the rate, and the way of how to utilize multiple light sources has great impact on the performance. In particular, simultaneous power division usage of multiple light sources through user grouping and power allocation brings almost no gain as compared with the case of single light source. On the other hand, time division usage of multiple light sources is capable of compensating for the hardware deficiency and thus increasing the rate greatly. It is found that OMC is not only superior to the conventional scheme with nonadjustable channel gains but also outperforms free space optical scheme at high signal-to-noise ratio region.

1. Introduction

Increasing the network throughput for diverse applications is always one of the main objectives of mobile communication systems. In the fifth-generation (5G) mobile communication system [1], the data rate can be boosted by three ways in the physical layer. Firstly, new spectrum with higher frequency, i.e., the millimeter wave band, is allocated to provide high-speed data rate links [2, 3]. Secondly, spatial multiplexing gain or the multiuser diversity gain is exploited, with massive multiple input multiple output (MIMO) or small cells to provide manyfold increase in data rate compared to conventional techniques with few antennas or large cells [4, 5]. In particular, with massive MIMO, the base station can generate multiple narrow beams for each user such that the emitted energy from transmit antennas can be conveyed much precisely, gaining very high spectral and energy efficiency. The third way is to utilize new capacity-approaching channel codes [6, 7] and nonorthogonal multiple access techniques [8, 9]. As the standardization process of 5G phase 2 has come to closure, researchers have begun to shift their research attention to the next-generation or the sixth-generation (6G) mobile communication system [10]. Although there is no official definition for 6G, some common views on it have been gradually reached [11–13]. An important view is that 6G will exploit full spectrum, spanning from radio frequency and millimeter wave to terahertz, visible light, and even higher frequency bands, to support full coverage communications ranging from terrestrial to ocean surface, air, and even space. It can be foreseen that high frequency electromagnetic wave including optical band will be utilized by 6G to achieve unprecedented data rate. To

our understanding, the optical band will not be used merely as the wireless backhaul or in fiber links. More desirably, it can be utilized to support fiber-like wireless access for multiple mobile users in the radio access network, which may be termed as optical mobile communication (OMC) [14]. OMC may trigger many new and exciting applications such as mobile virtual reality. It also provides a handy carrier for future wireless quantum direct communication in the optical band with coherent processing [15].

OMC can be regarded as an alternative implementation of massive MIMO in two aspects [10]. Firstly, OMC may exploit one or more spatial light modulators (SLMs) for beam steering. Each SLM consists of a large number (possibly a few million) of optical elements such as liquid crystals which can be viewed as massive antennas. Secondly, the energy is concisely distributed and delivered to desired users with very thin laser beams, and there is little leakage in other spatial directions. Nonetheless, the optical band devices are not bulky and of low power consumption. Therefore, OMC is an alternative substitute of massive MIMO in the optical band. As a special variant of optical wireless communication (OWC), OMC also faces many physical limitations, e.g., the optical beam may be easily blocked by obstacles like buildings or attenuated in adverse weather. Therefore, it is more likely that OMC will find its role as a complementary technique for existing mainstream wireless communications to provide very high-speed peak data rate links in some future mobile communication scenarios.

It should be noted that there are several other OWC techniques that can support mobile access for multiple users utilizing light spectrum, including infrared communication (IR), visible light communication (VLC), and free-space optical (FSO) communication [16]. For example, [17, 18] studied the throughput performance of mobile users in VLC systems. The mobility is guaranteed by utilizing wide half-power semiangle light emitting diodes (LEDs) as light sources. Multiple light sources is used to further enhance the light coverage probability. In other words, wide beams are projected in VLC to support mobility, which is also the case in IR. OMC differs from VLC and IR in that it concentrates the optical power on the receiver side, which is more energy efficient. In addition, the signal processing in LED-based VLC is inherently noncoherent, whereas OMC can be both noncoherent or coherent, depending on how to perform modulation in the laser source. In this work, coherent processing is considered. OMC is also different from conventional FSO communication in that it is designed to accommodate multiuser mobile communication, where the users may not be covered by a single wide beam spot, and the number and locations of users may change from time to time. Therefore, flexible beam splitting and steering are the key enabling function and feature of OMC system, which bring larger achievable rate region than current OWC schemes.

Realizing OMC is quite challenging, and many technical and engineering issues must be resolved. For instance, due to cost and scalability concerns, it is impractical to equip a large number of laser devices to accommodate multiple users. Instead, flexible beam splitting and steering for a single laser beam must be dealt with. [19] proposed to use liquid crystal SLM for beam adaptation among other potential techniques such as digital micromirror device (DMD) to support infrastructure-to-vehicle (I2V) communication. Experimental results verified the feasibility of beam adaptation. Rate region for unicast downlink communication was derived for a two-user system with orthogonal and nonorthogonal multiple access techniques. However, the rate region only depicted the scenario of motionless users. [20, 21] investigated more practical scenarios with user mobility for coherent and noncoherent transmissions, respectively. Many new factors, such as the beam length, the communication time (ON-state), and the power split ratio, must be configured in a joint manner to achieve the best potential performance. This paper extends the results in [20] to multiple light sources which bring new design freedom and challenges. As OMC is still in its infancy, in this work, we focus on the information theoretic aspects of the system. Although coherent processing is much more challenging in system implementation as compared with noncoherent schemes, we study the system performance under this assumption to unveil the maximum potential gain of OMC over the conventional schemes and to identify the key factors that affect the gain. In fact, considerable advancements have been achieved in recent years for coherent optical wireless access [22–24], even in communication with satellite [25]. Thus, OMC with coherent transmission and processing can be expected in the future.

Resource allocation is among the key issues in other OWC schemes with user mobility, such as in VLC [26–28]. In those systems, the optimal resource allocation is in general hard to derive, and suboptimal solutions were proposed. Similar situations are found in this work; however, the task in OMC is systematically different from those works, since the light sources, including SLM, have very different physical models as compared to other systems. Therefore, the optimization process is fundamentally different from existing works.

With this regard, this paper comprehensively investigates the achievable rate performance of broadcast OMC system with multiple mobile users. The contributions of this paper are summarized as follows:

(i) This paper considers two scenarios of broadcast OMC. As a basis, in the first scenario, a single light source with multiple mobile users is considered. In this scenario, the impacts of user mobility and the switch time of SLM on the achievable rate performance is the key issue, which has not been addressed previously. In the second scenario, besides user mobility, multiple light sources are involved and share the total transmit power. The main challenges include how to efficiently coordinate the usage of multiple light sources and the associated optimal resource allocation strategies, which are also not studied in current literature

(ii) To address the issue in the first scenario, we set the reflected beams to be rectangular to provide consistent communication links as users move. The beam

length for each user is optimally selected according to user's speed. Then, the optimal period of the ON-state of SLM and the optimal power allocation ratios among users are jointly optimized. Based on the analysis, the rate region of a two-user system is depicted, and then, the maximum common rate is obtained

(iii) To address the challenges in the second scenario, we distinguish and study power division usage of multiple light sources and time division usage of multiple light sources, respectively. In power division mode, users are grouped, and each group is served by a light source. A simple user grouping strategy as well as a user group power allocation algorithm is proposed. The user grouping strategy is proved to be optimal at low signal-to-noise ratio (SNR) regime. In time division mode, light sources take turns to serve all users. The optimal serving period of each light source is derived in closed form. It is found that time division usage of multiple light sources is more beneficial as compared to power division usage of multiple light sources as well as two benchmark schemes, i.e., the conventional scheme with nonadjustable channel gains and the FSO scheme

The remaining of this paper is organized as follows. Section 2 provides the system model with a single light source whose beam is adapted by an SLM. The corresponding performance is analyzed in Section 3. Then, Section 4 and Section 5 investigate how to exploit multiple light sources in power division and time division manners, respectively. Various numerical results are provided in Section 6. Finally, conclusions are drawn in Section 7 with some discussions on future research directions.

2. System Model with a Single Light Source

This section reviews briefly the principle of OMC with a single light source and exemplifies it in I2V broadcast communication with user mobility.

2.1. OMC Principle. The basic approach of OMC is to split a single narrow optical beam generated by a laser device into multiple wider beams and steer those beams to desired and in general different spatial directions, realized by a beam splitting and steering device. In [19], SLM was employed to accomplish the task of flexible beam splitting and steering. Other options were also discussed therein. SLM can be viewed as an optical massive MIMO device which is capable of finely tuning the phase of the wave front of an input laser beam. By properly setting the control or address signal for the SLM, the wave front of the input laser beam will be manipulated into a hologram signal by the SLM. This hologram is then transformed to an image and projected onto a larger area by a lens system. The hologram is fully determined by the address signal fed to the SLM, and it also determines the image through the mapping of two-dimensional fractional Fourier transformation. Therefore, the image can be tuned flexibly and usually consists of several beam spots for user coverage in OMC.

Mathematically, the above operations are equivalent to splitting an optical signal $x(t)$ of power P into K beams with possibly different crosssection shapes. Beam k serves user k and can be represented by $x_k(t) = \sqrt{\alpha_k}x(t)$. It has power P_k which is a fraction of the total power, i.e., $P_k = \alpha_k P$, where $0 \le \alpha_k \le 1$ and $\sum_{k=1}^{K} \alpha_k = 1$ without considering the power loss in the beam splitting phase. The key feature of OMC lies in that K and α_k are tunable, which is in contrast with the conventional beam adaptation technique based on the commonly used beam splitter, since beam splitter can only split a beam into two with a fixed power ratio after it has been fabricated. This implies that the communication channel in OMC is tunable or controllable to a large extent. Based on the above mathematical principle, the aim of this paper is to analyze the potential performance of OMC and compare it with existing schemes. Implementation issues, including the beam adaptation schemes and demo, positioning and coherent transmitting and receiving techniques, and their feasibilities, can be found in [19, 29, 30]. Improved or new implementations will be developed in future works.

2.2. OMC in I2V Broadcasting with User Mobility. I2V communication is among the key enabling technologies for realizing Internet of Vehicles (IoV) and Internet of Things (IoT). In this paper, I2V broadcasting scenario is considered to reveal the potential of OMC, which is shown in Figure 1. Herein, the transmitter side is attached on the infrastructure such as a lamp post, which is usually within 10 meters in height. The wavelength of the light source does not affect the signal model; thus, infrared light can be utilized in this scenario. However, it should be noted that OMC can be applied in broader applications such as in industrial environment where human eye safety is not a concern. The transmitter generates an image which consists of several beam spots for multiple vehicles (users) in a certain area after the image is projected by a lens system. The beams bear the same information that is common for all users. Here, we denote the original electrical domain information as $\sqrt{P}x$, where x is the random information symbol that has zero mean and unit variance, and P is the power of the signal. Each beam may be allocated with different power and crosssection shapes according to the user mobility behaviours. Suppose there are K users in total and user k has a speed of v_k and is allocated power $P_k = \alpha_k P$ in its associated beam. The receiver can be attached on the roof of the vehicle to receive the broadcasted information when it is covered by a beam.

An important limitation of adopting SLM for beam adaptation is that the image cannot be changed continuously in time. In contrast, to change from a current image to another, a switch time Δt to fully reload the new address signal and regenerate the new image is required for the SLM. Commercially available SLMs have a minimum switch time in the order of several milliseconds. This hardware phenomena prevents the most efficient beam adaptation scheme that

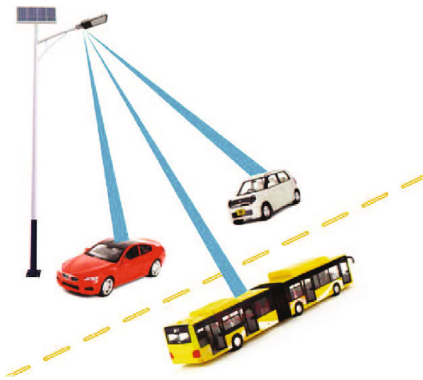

Figure 1: Illustration of I2V broadcasting scenario of OMC with user mobility.

the receiver aperture is persistently covered and tracked by a very narrow beam. Instead, the beams generated by a realistic SLM have to be wide enough to support continuous link coverage with user mobility for a communication ON-state of duration T. When the vehicles move out of the current beam coverage area, switch is triggered to regenerate a new beam pattern to recover the links, resulting in an OFF-state of duration Δt. Figure 2 illustrates the beam adaptation process for user k. Initially at time $t = 0$, a beam is generated to cover the expected path of the receiver aperture. The shape of the beam is set as a rectangular with length L_k and survives for a time duration T. The width of the beam is a bit larger than the size of the receiver aperture, which is assumed to be a square of length D for simplicity. At time $t = T$, the SLM enters a switch state, and the beam diminishes for a time duration of Δt. Then, at $t = T + \Delta t$, a new beam is established and the communication link recovers.

With the above description, the received downlink electrical domain signal of user k after coherent receiving can be written as

$$x_k = R_{\text{rec}} \sqrt{c_k P_{\text{LO},k} \alpha_k P \frac{D}{L_k}} x + z_k, \tag{1}$$

where R_{rec} is the responsivity of the receiver detector, $P_{\text{LO},k}$ denotes the power of the local oscillator, and z_k is the noise component. With coherent detection, the main contribution of the aggregate noise z_k in (1) comes from the shot noise in the local oscillator. According to [31], z_k can be modeled as complex Gaussian with zero mean and variance σ_n^2. The coefficient c_k accounts for several nonideal factors affecting the link budget, including the loss in signal propagation, the never-collected power owing to the larger width of the beam over the receiver aperture length D, and the possible power loss due to the pointing error of the aperture toward the incident beam direction. Since the communication distance is relatively short in the studied scenario for laser beams, for simplicity and without loss of generality, c_k is set as 1 in this paper, as both the fading effect and power attenuation due to atmospheric turbulence and distance-dependent power decay are negligible in such a limited range [32, 33]. On the other hand, if atmospheric turbulence and distance-dependent power decay are considered in long distance communication, they must be reflected in c_k. This is beyond the scope of this paper and will be studied in the future. $R_{\text{rec}}\sqrt{P_{LO,k}}$ is also assumed to be unity here. Thus, the effective received SNR is given by $\alpha_k PD/L_k\sigma_n^2$. Finally, we note that x_k in (1) is effective only in the time duration of $[0, \min\{T, (L_k - D)/v_k\}]$ over a full time cycle of $(T + \Delta t)$, where $(L_k - D)/v_k$ is the maximum time duration for the receiver aperture to be fully covered by a beam spot as it moves forward. Therefore, according to Shannon's capacity formula [34], the effective achievable rate (with unit of bits/s/Hz) of user k, averaged in the whole time duration of $(T + \Delta t)$, can be expressed as

$$R_k(L_k, \alpha_k, T, v_k) = \frac{\min\{T, (L_k - D)/v_k\}}{T + \Delta t} \log_2\left(1 + \frac{\alpha_k PD}{L_k\sigma_n^2}\right), \tag{2}$$

which is related to a bunch of parameters. In particular, L_k, α_k, and T are not hardware determined and must be optimized according to other fixed parameters, such as Δt and v_k. The optimization goal is to maximize the minimum value of $\{R_k\}_{k=1}^K$ for a given total power P. The case of single light source is considered in Section 3, while the case of multiple light sources will be studied in Sections 4 and 5.

3. Rate Maximization

3.1. Beam Length Optimization. In this section, we investigate the best option for the beam length L_k. This issue arises from the fact that a larger L_k results in a longer communication time, but a reduced instantaneous power, while a smaller L_k results in a shorter communication time, but a more concentrated received power. It is thus desired to optimize L_k for rate maximization. To do this, we first note that $L_k \geq D$ for a full coverage of the receiver aperture. Moreover, $(L_k - D)$ should be no larger than $v_k T$; otherwise, there will be a portion of $(L_k - D - v_k T)/L_k$ transmitted power that will never be collected for usage. Note that in practical system, it is desired that a longer L_k than assumed here is configured for robustness purpose. Thus, $L_k \leq v_k T + D$ and

$$R_k(L_k, \alpha_k, T, v_k) = \frac{(L_k - D)/v_k}{T + \Delta t} \log_2\left(1 + \frac{\alpha_k PD}{L_k\sigma_n^2}\right). \tag{3}$$

The problem is to find the optimal $L_k \in [D, v_k T + D]$ to maximize R_k in (3). Note the fact that

$$\begin{cases} \left.\dfrac{\partial R_k}{\partial L_k}\right|_{L_k = D} > 0, & \left.\dfrac{\partial R_k}{\partial L_k}\right|_{L_k \longrightarrow \infty} = 0, \\ \dfrac{\partial^2 R_k}{\partial^2 L_k} < 0, & \forall L_k \geq D, \end{cases} \tag{4}$$

which indicates that R_k in (3) is an increasing function of L_k. Therefore, the optimal L_k must be $L_k^* = v_k T + D$, and the corresponding rate is reduced to

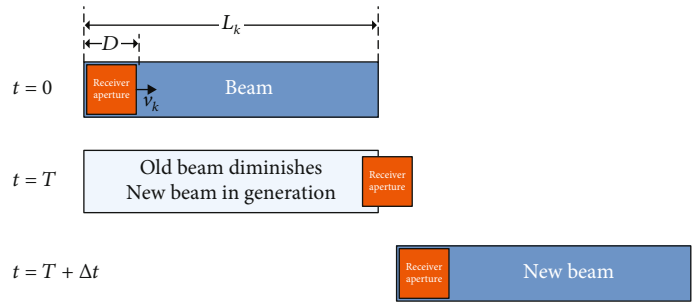

Figure 2: Snapshots of beam adaptation for user k.

$$\bar{R}_k(\alpha_k, T, v_k) = \frac{T}{T+\Delta t}\log_2\left(1+\frac{\alpha_k D\gamma}{v_k T + D}\right), \tag{5}$$

where $\gamma = P/\sigma_n^2$ is defined as the transmit SNR.

3.2. Rate Region of Two-User System. In this subsection, we investigate the rate region of a two-user system by optimizing the power split ratios $\alpha_1, \alpha_2, \cdots, \alpha_K$ and the communication time T. The result provides a simple yet relatively complete picture of OMC and reveals its potential gain with "controllable" channel over conventional fixed channel. Firstly, note that the maximum rate of user k is achieved only when $\alpha_k = 1$, i.e.,

$$\tilde{R}_k(T, v_k) \triangleq \max_{\{\alpha_k\}} \bar{R}_k(\alpha_k, T, v_k) = \bar{R}_k(1, T, v_k), \tag{6}$$

which is still a function of T. Here, $\triangleq$ denotes definition. There is no analytical expression for the optimal T. However, we have the following proposition.

Proposition 1. *$\tilde{R}_k(T, v_k)$ is unimodal with respect to T for $T \in (0,\infty)$.*

Proof. see Appendix A.

Therefore, any efficient line search method can be used to obtain the optimal T very quickly. Assume that the maximal rate is given by

$$\tilde{R}_k^*(v_k) \triangleq \max_{\{T\}} \tilde{R}_k(T, v_k) = \tilde{R}_k(T_k^*, v_k), \tag{7}$$

achieved at $T = T_k^*$, for $k = 1, 2$. Note that T_k^* and thus $\tilde{R}_k^*(v_k)$ are only related to a specific k. In addition, in Proposition 1, $\alpha_k = 1$ is set only to help to find a vertex of the rate region boundary. In general case, α_ks are less than 1 to ensure all users have positive rates, as will be elaborated in Section 3.3. The problem of finding a specific point (r_1, r_2) on the boundary of the rate region can now be formulated as

$$\text{(P1)}: r_2 = \max_{\{\alpha_2, T\}} \bar{R}_2(\alpha_2, T, v_2), \tag{8}$$

$$\text{s.t.} \begin{cases} \bar{R}_1(1-\alpha_2, T, v_1) = r_1, \\ 0 \le \alpha_2 \le 1, \end{cases} \tag{9}$$

where r_1 is a given value in the range of $[0, \tilde{R}_1^*(v_1)]$. Using the first constraint, we obtain

$$\alpha_2 = 1 - \frac{\left(2^{(r_1(T+\Delta t))/T} - 1\right)(v_1 T + D)}{D\gamma}. \tag{10}$$

Then, we can transform the objective function to

$$r_2 = \max_{\{T\}} \check{R}_2(T, v_2), \tag{11}$$

where

$$\check{R}_2(T, v_2) \triangleq \bar{R}_2\left(1 - \frac{\left(2^{(r_1(T+\Delta t))/T} - 1\right)(v_1 T + D)}{D\gamma}, T, v_2\right), \tag{12}$$

which is also a function of T. Again, we have the following proposition. □

Proposition 2. *$\check{R}_2(T, v_2)$ is unimodal for $T \in [T_L, T_U]$, where the domain of definition for T is determined by the constraint $0 \le \alpha_2 = 1 - ((2^{(r_1(T+\Delta t))/T} - 1)(v_1 T + D)/D\gamma) \le 1$.*

Proof. α_2 in (10) is a function of T and is always no greater than 1 for $T > 0$. It can be shown that the second-order derivative of $\alpha_2(T)$ with respect to T is always positive, and thus, $\alpha_2(T)$ is a concave function. When T approaches 0 and infinity, $\alpha_2(T)$ approaches negative infinity. Therefore, there must exist two points T_L and T_U, $0 < T_L \le T_U < \infty$, such that for any $T \in [T_L, T_U]$, $0 \le \alpha_2 \le 1$. The remaining proof is similar to that for Proposition 1 and is omitted here.

Assuming the optimal $\check{R}_2(T, v_2)$ is given by $r_2 = \max_{\{T\}} \check{R}_2(T, v_2) = \check{R}_2(\check{T}, v_2)$ achieved at $T = \check{T}$, where $\check{T}$ is related to both users' parameters, we can obtain all pairs of (r_1, r_2) that constitute the boundary of the rate region. □

3.3. Maximum Rate. In broadcast applications, we are more concerned with the minimum rate of all users and want to maximize this minimum rate. In OMC, this task is easy to realize since the power ratios α_k, $k = 1, 2, \cdots, K$, are adjustable: regardless of the moving speeds, higher rate users should "slice" a certain portion of their allocated power to the low rate users until all users have the same data rate.

We refer to the rate of equilibrium as the maximum rate $R^*(\mathbf{v})$ here, which is just the maximum of the minimum rate among all users, where $\mathbf{v} = [v_1, v_2, \cdots, v_K]^T$. To find $R^*(\mathbf{v})$ and its associated optimal power allocation ratios and communication time T, we set

$$\bar{R}_1(\alpha_1, T, v_1) = \cdots = \bar{R}_K(\alpha_K, T, v_K), \tag{13}$$

which brings $\alpha_k = ((v_k T + D)/(v_1 T + D))\alpha_1$. Combining $\sum_{k=1}^{K} \alpha_k = 1$, the optimal power allocation ratios can be found as

$$\widehat{\alpha}_k = \frac{v_k T + D}{vT + KD}, \tag{14}$$

which is a function of T as well as all users' speeds through $v = \sum_{k=1}^{K} v_k$. Generally speaking, a user with high mobility should be allocated more power to achieve the rate balance. Substitute (14) into (13), we get

$$R^*(\mathbf{v}) = \max_{\{T\}} \bar{R}_k(\widehat{\alpha}_k, T, v_k) = \max_{\{T\}} \frac{T}{T + \Delta t} \log_2\left(1 + \frac{D\gamma}{vT + KD}\right), \tag{15}$$

which has the same structure as (6) and is thus unimodal according to Proposition 1. Again, the optimal T^* that maximizes $R^*(\mathbf{v})$ in (15) has no analytical expression and has to be obtained through numerical methods.

4. Power Division Usage of Multiple SLMs

As the number of users gets larger and their speeds vary in a wider range, setting a common communication period T^* for all users may decrease the overall achievable rate. A natural remedy is to employ multiple laser sources and, correspondingly, multiple SLMs to serve the users. In this scenario, we consider a single base station consisting of multiple laser sources. Each laser source is associated with a single SLM, forming a laser-SLM pair. On one hand, a laser-SLM pair will serve a group of users as if in the single SLM case; however, all laser sources in the base station must share a total transmit power budget. On the other hand, different SLMs serving different user groups can be configured with unequal communication periods now, leading to new design freedom and potential performance gain. For notational simplicity, in the following, we use multiple SLMs to represent multiple laser-SLM pairs. We refer to this scenario as power division usage of multiple SLMs. The key problems include how to group the users and allocate powers among user groups.

4.1. Problem Statement. Assume there are N available SLMs in the OMC system, where we only consider the nontrivial case $1 < N < K$. Each SLM is allocated a fraction of total power given by $\beta_n P$, where $0 < \beta_n < 1$, $\sum_{n=1}^{N} \beta_n = 1$, and serves a group of users whose indices form a set $\mathcal{K}_n$ with cardinality $|\mathcal{K}_n|$, where $|\mathcal{K}_n|$ satisfies $1 \le |\mathcal{K}_n| < K$, $\sum_{n=1}^{N} |\mathcal{K}_n| = K$. Each group of users behave just like the single SLM case in Section 3, i.e., through proper power allocation among those users, denoted as $\alpha_{n_m}\beta_n P$, where α_{n_m}, $m = 1, 2, \cdots, |\mathcal{K}_n|$, is the allocated power ratio of the mth user in this group satisfying $\sum_{m=1}^{|\mathcal{K}_n|} \alpha_{n_m} = 1$; they eventually approach a maximum rate for some optimal T_n^* that is common for all users in this group. Different groups in general have different optimal T_n^*. Therefore, for ease of user scheduling, it is assumed here that each SLM serves only a single group of users and each group of users are served by a single SLM.

The problem is to find the optimal grouping strategy $\{\mathcal{K}_n\}_{n=1}^{N}$ at the transmitter side, along with optimal power allocation among groups and users, i.e., $\{\beta_n\}_{n=1}^{N}$ and $\{\alpha_{n_m}\}_{m=1}^{|\mathcal{K}_n|}$, $n = 1, 2, \cdots, N$, as well as optimal transmission time $\{T_n^*\}_{n=1}^{N}$ for each group, to maximize the common rate of all users.

4.2. Optimal Power Allocation for Given User Grouping. Firstly, we investigate how to optimally allocate power to each group and user for a *given* user grouping result. For users in group n, their rate should be the same by proper power allocation. Therefore, according to Section 3.3, the optimal power allocation ratios are given by

$$\alpha_{n_m} = \frac{v_{n_m} T_n + D}{\left(\sum_{m=1}^{|\mathcal{K}_n|} v_{n_m}\right) T_n + |\mathcal{K}_n| D}, \tag{16}$$

which results in the rate of this group as

$$\mathcal{R}_n(T_n, \beta_n) = \frac{T_n}{T_n + \Delta_t} \log_2\left(1 + \frac{\beta_n D\gamma}{\left(\sum_{m=1}^{|\mathcal{K}_n|} v_{n_m}\right) T_n + |\mathcal{K}_n| D}\right). \tag{17}$$

The remaining problem can be formulated as

$$\text{(P2)}: \{T_n^*, \beta_n^*\}_{n=1}^{N} = \arg \max_{\{T_n, \beta_n\}_{n=1}^{N}} \mathcal{R}_1(T_1, \beta_1), \tag{18}$$

$$\text{s.t.} \begin{cases} \mathcal{R}_n(T_n, \beta_n) = \mathcal{R}_1(T_1, \beta_1), n = 2, 3, \cdots, N, \\ \sum_{n=1}^{N} \beta_n = 1. \end{cases} \tag{19}$$

Proposition 3. *There is a unique solution to problem (P2) for a given user grouping result.*

Proof. Due to the unimodal property of $\mathcal{R}_n(T_n, \beta_n)$ with respect to T_n for any given β_n, the optimal T_n is a function of β_n and must be the point which maximizes $\mathcal{R}_n(T_n, \beta_n)$. Otherwise, a portion of power is not fully exploited and can be sliced and distributed to all users to further increase the common rate. Denoting $\tilde{\mathcal{R}}_n(\beta_n) = \max_{T_n} \mathcal{R}_n(T_n, \beta_n)$, the constraints are changed to $\tilde{\mathcal{R}}_n(\beta_n) = \tilde{\mathcal{R}}_1(\beta_1)$, $\forall n$, and $\sum_{n=1}^{N} \beta_n = 1$. As $\tilde{\mathcal{R}}_n(\beta_n)$ is an increasing function of β_n, there exists only a single β_n that satisfies the constraint $\tilde{\mathcal{R}}_n(\beta_n)$

Input: $\{\mathscr{K}_n\}_{n=1}^N$ (with associated parameters $K, N, |\mathscr{K}_n|, v_n, n = 1, 2, \cdots, N$), Δ_t, γ, D, and precision ε.
Output: the maximum common rate $\mathscr{R}^*$ and its associated power allocation $\{\beta_n^*\}_{n=1}^N$, $\{\alpha_{n_m}\}_{m=1}^{|\mathscr{K}_n|}$, $n = 1, 2, \cdots, N$.
Initialize: $\beta_n = 1/N, n = 1, 2, \cdots, N$, $tol = 10\varepsilon$.
1: **while** $tol > \varepsilon$ **do**
2: **for** $n = 1 : N$ **do**
3: Set α_{n_m} using (16);
4: Find $\tilde{\mathscr{R}}_n(\beta_n)$ by optimizing T_n in (17).
5: **end for**
6: Set $\mathscr{R}_{\min} = \min\{\tilde{\mathscr{R}}_n(\beta_n), n = 1, 2, \cdots, N\}$;
7: Record $n_{\min}$ satisfying $\tilde{\mathscr{R}}_{n_{\min}}(\beta_{n_{\min}}) = \mathscr{R}_{\min}$.
8: Set $\mathscr{R}_{\max} = \max\{\tilde{\mathscr{R}}_n(\beta_n), n = 1, 2, \cdots, N\}$;
9: Update $tol = (\mathscr{R}_{\max} - \mathscr{R}_{\min})/\mathscr{R}_{\min}$.
10: **for** $n = 1 : N$ except for $n_{\min}$
11: Decrease β_n until $\tilde{\mathscr{R}}_n(\beta_n) = \mathscr{R}_{\min}$.
12: **end while**
13: Update $\beta_n = \beta_n / \sum_{i=1}^{\beta_i} \beta_i$, $n = 1, 2, \cdots, N$.
14: **end while**
15: Set $\mathscr{R}^* = \mathscr{R}_{\min}$, $\beta_n^* = \beta_n$, $\alpha_{n_m}^* = \alpha_{n_m}$, $\forall n, m$, and output.

Algorithm 1: Proposed group and user power allocation scheme for given user grouping

$= \tilde{\mathscr{R}}_1(\beta_1)$, i.e., β_n is a bijective function of β_1 and can be denoted as $\beta_n = B_n(\beta_1)$. Furthermore, when β_1 increases, $\tilde{\mathscr{R}}_1(\beta_1)$ increases and so does β_n, which means $B_n(\beta_1)$ is an increasing function of β_1. As a consequence, $B(\beta_1) = \beta_1 + \sum_{n=2}^N B_n(\beta_1)$ is an increasing function of β_1, and thus, $B(\beta_1) = 1$ has only a single (and thus optimal) solution β_1^*, implying there is also a single solution for $\{\beta_n, T_n\}_{n=1}^N$, which proves Proposition 3. □

Based on the above proof, we can conclude that the maximum common rate can be obtained by searching the optimal β_1 such that $B(\beta_1) = 1$ is satisfied. Noting $B(\beta_1)$ is a monotonic increasing function, here, we propose an efficient and optimal power allocation method to find the maximum common rate, which is shown in Algorithm 1.

In the procedure of Algorithm 1, step 11 forces the rate of all groups to be equal by slicing down the power of the groups that has larger rate than $\mathscr{R}_{\min}$. While this guarantees the rate of all groups to be equal, it does not fully utilize the available power. Therefore, step 13 lifts up the power split ratio β_n for all groups through normalization. We can observe that the minimum group rate is increasing for each additional iteration. Upon convergence, the two constraints in problem (P2) are automatically satisfied within numerical precision, indicating the resultant solution is optimal according to Proposition 3. Note that Algorithm 1 only involves a series of one-dimensional line search for unimodal functions instead of exhaustive search, which is efficient.

4.3. Suboptimal User Grouping. In this subsection, we investigate the remaining issue of user grouping. The number of all feasible grouping results is referred to as Stirling's number of the second kind [35], denoted by $S(K, N)$, which grows very fast as K increases and N is not close to 1 nor K. For instance, $S(16, 4) \approx 1.71 \times 10^8$ and $S(20, 8) \approx 1.52 \times 10^{13}$. This means the brute-force searching method is impractical here even for a medium K. Therefore, to assess the performance gain of using multiple SLMs, we have to seek some suboptimal strategies that have affordable computational complexities. In this section, we propose a heuristic user grouping strategy. The intuition is that users with lower speeds consume much less power such that we may allocate more power to poor users with higher speeds to improve their performance. Specifically, the proposed user grouping strategy is as follows: assuming the K users are sorted by their speeds: $v_1 \le v_2 \le \cdots \le v_K$, the user grouping strategy is given by $\mathscr{K}_n = \{n\}$, for $n = 1, 2, \cdots, N-1$, and $\mathscr{K}_N = \{N, N+1, \cdots, K-1, K\}$, which needs no specific calculations.

Proposition 4. *The proposed user grouping strategy is asymptotically optimal in the low SNR regime.*

Proof. see Appendix B. □

5. Time Division Usage of Multiple SLMs

As will be seen through simulations in 6.3, quite unexpectedly, power division usage of multiple SLMs, even in the extreme case of K SLMs, does not bring noticeable performance gain as compared with the case of single SLM. Therefore, it is desired to further find better means to fully exploit the additional SLMs to enhance the performance in practice. In power division usage of multiple SLMs, each user will experience link break during the OFF-state of its serving SLM, which lasts at least Δt seconds. This is an important factor that limits the rate performance. Motivated by this, we consider time division usage of multiple SLMs in which the SLMs take turns to communicate with all users such that

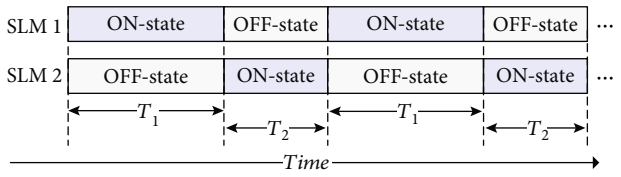

Figure 3: Illustration of the state changes in time division usage of two SLMs.

the users always receive light power without break. Figure 3 shows the states of two SLMs.

Basically, each SLM's ON-state will just cover other's OFF-state in an alternating manner. The period of OFF-state must be at least Δt. In each SLM's ON-state, it occupies the full power and serves all users with proper power allocation but without user grouping. Then, with a similar approach in 3.3 the maximum common rate can be rewritten as

$$\begin{aligned} \mathrm{R}^*(\mathbf{v}) = \max_{\{T_1,T_2\}} & \frac{T_1}{T_1+T_2}\log_2\left(1+\frac{D\gamma}{vT_1+KD}\right) \\ & + \frac{T_2}{T_1+T_2}\log_2\left(1+\frac{D\gamma}{vT_2+KD}\right). \end{aligned} \tag{20}$$

The constraints are $T_1 \geq \Delta t$ and $T_2 \geq \Delta t$ to cover the minimum switch time. Generalizing to N SLMs, the rate changes to

$$R^*(\mathbf{v}) = \max_{\{T_1,\cdots,T_N\}} \frac{1}{T}\sum_{n=1}^{N} T_n \log_2\left(1+\frac{D\gamma}{vT_n+KD}\right), \tag{21}$$

where $T = \sum_{n=1}^{N} T_n$ and the constraints are $\sum_{l\neq n} T_l = T - T_n \geq \Delta t$, $n = 1, \cdots, N$, which means each SLM's OFF-state period will be fully covered by adding all the other SLM's ON-state periods. Denote $a_n = T_n/T$, $\forall n$, the rate becomes

$$R^*(\mathbf{v}) = \max_{\{a_1,\cdots,a_N\}} \sum_{n=1}^{N} a_n \log_2\left(1+\frac{D\gamma}{vTa_n+KD}\right), \tag{22}$$

with constraints $\sum_{n=1}^{N} a_n = 1$, $a_n > 0$, and $T(1-a_n) \geq \Delta t$, $\forall n$. It can be shown that $R^*(\mathbf{v})$ is maximized when $T = (N/(N-1))\Delta t$ and $a_n = 1/N$, $\forall n$, and the rate is given by

$$R^*(\mathbf{v}) = \log_2\left(1+\frac{D\gamma}{(v\Delta t/(N-1))+KD}\right), \tag{23}$$

which is an increasing function of N for $N \geq 2$. When N approaches to infinity, $R^*(\mathbf{v})$ achieves its upper bound as

$$R_{UB} \triangleq \lim_{N\longrightarrow\infty} R^*(\mathbf{v}) = \log_2\left(1+\frac{\gamma}{K}\right). \tag{24}$$

It is worth noting that this upper bound can also be achieved with a single SLM system if the switch time Δt approaches to *zero*, as indicated by (5). Therefore, (24) implies that utilizing unlimited number of SLMs completely eliminates the adverse effect of switch time due to hardware limitation. However, in practice, it is more appropriate to use as less SLMs as possible to reduce the implementation difficulty in coordinating different SLMs and to improve the robustness of the system. From this perspective, $N = 2$ would be a good tradeoff between complexity and performance. In this case, the rate is given by

$$R^*(\mathbf{v}) = \log_2\left(1+\frac{D\gamma}{v\Delta t+KD}\right). \tag{25}$$

It can be inferred from (25) that when $v \longrightarrow 0$ with motionless users, or $\Delta t \longrightarrow 0$ with advancement in hardware production, the rate can also approach its upper bound R_{UB} even there are only two SLMs.

Since additional SLMs are utilized to reduce the adverse effect of switch time, the rate performance is expected to outperform that of power division usage of SLMs described in 4. In addition, it avoids user grouping and the corresponding power allocation among groups, which has much lower system complexity and can be viewed as a stronger candidate for practical OMC implementations.

6. Numerical Results

This section provides various numerical results of the rate maximization in OMC and compares them with other benchmark schemes. Subsections 6.1 to 6.2 provide results with single SLMs, while subsection 6.3 illustrates the results with multiple SLMs. Two benchmark schemes are considered here.

(1) The first benchmark scheme can also split and steer the beam but with fixed power allocation ratios (thus, this scheme is denoted as "fixed-PA" in the legends) for different users; thus, its effective channel gains are nonadjustable as compared with OMC. We assume equal power allocation here. This scheme may represent the conventional beam adaption scheme using beam splitter but with enhanced capability of steering the beams to different users freely. The purpose is to evaluate the gain brought by adaptive power allocation according to users' speeds in OMC

(2) The second benchmark scheme is an FSO scheme (denoted as "FSO" in the legends) in time division mode, in which the single beam can track a single user precisely at any time interval with all power allocated to and focused on that user. Users are served in a time division manner with zero switch time. Thus, the rate for such an idealized system is simply given by

$$R^*_{\mathrm{FSO}} = \frac{1}{K}\log_2(1+\gamma). \tag{26}$$

When there are multiple SLMs, the rate of user group n is given by

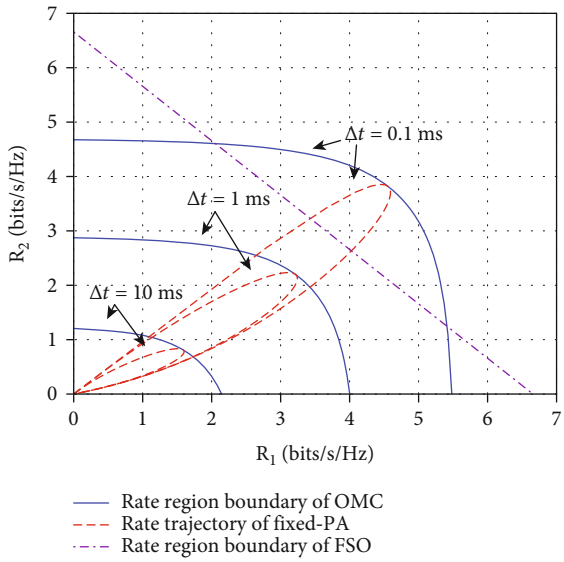

Figure 4: Rate region of two-user system with different Δt.

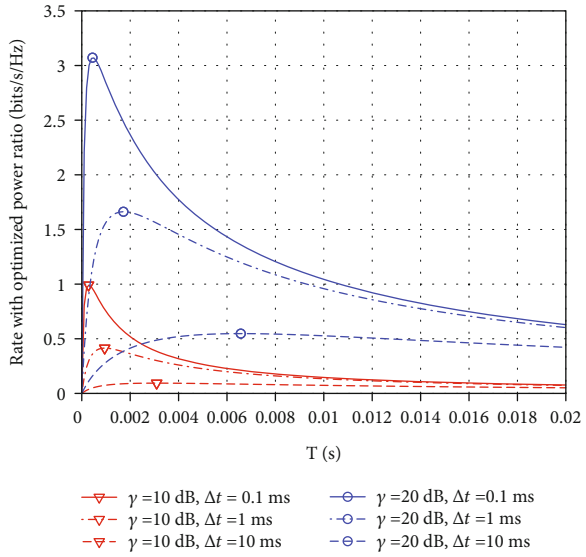

Figure 5: Rate curves as a function of T with optimized power split ratio

$$R^*_{\mathrm{FSO},n} = \frac{1}{|\mathscr{K}_n|} \log_2(1 + \beta_n \gamma). \tag{27}$$

If we treat $|\mathscr{K}_n|$, $n = 1, 2, \cdots, N$, as continuous variables, it would not be hard through convex optimization to prove that the optimal $|\mathscr{K}_n|$ is given by K/N and the optimal β_n is given by $1/N$. The corresponding rate is given by

$$R^*_{\mathrm{FSO}} = \frac{N}{K} \log_2\left(1 + \frac{\gamma}{N}\right), \tag{28}$$

for $N \leq K$, which can be viewed as an upper bound of the practical case in which $|\mathscr{K}_n|$, $n = 1, 2, \cdots, N$, are integers. Note that when $N = K$, the rate of FSO in (28) achieves its upper bound which is identical with the upper bound rate of OMC given by (24).

In the following, the size of the receiver aperture is set as $D = 1$ cm, which can be realized with large-aperture PD or through light concentration by a lens. The switch time of the SLM depends on the specific device and can be expected to improve in the future. In the following simulations, $\Delta t = 0.1$ ms, 1 ms, and 10 ms are involved to reveal its impact on the performance.

6.1. Rate Region of Two-User System. First, the rate region of a two-user system is given here. Figure 4 shows the rate region at SNR = 20 dB with different Δt. The speeds of the two users are set as $v_1 = 20$ Km/h and $v_2 = 80$ Km/h. Several facts can be observed in Figure 4. Firstly, in OMC and the fixed-PA schemes, the user with lower speed may achieve a larger maximum rate, which complies with the intuition. Secondly, with controllable channel management, the OMC scheme entitles much larger rate region than the fixed-PA scheme. In fact, in the fixed-PA scheme, the feasible rate pairs constitutes a trajectory rather than a region. Thirdly, Δt has great impact on the rate performance. With decreased Δt, the rate region is expanded. This indicates that, with advancement in manufacturing of SLM entitling much shorter switch time, higher rate OMC communication can be expected in the future. In fact, it can be seen that with smaller switch time, part of the rate region of OMC lies outside of that of the FSO scheme.

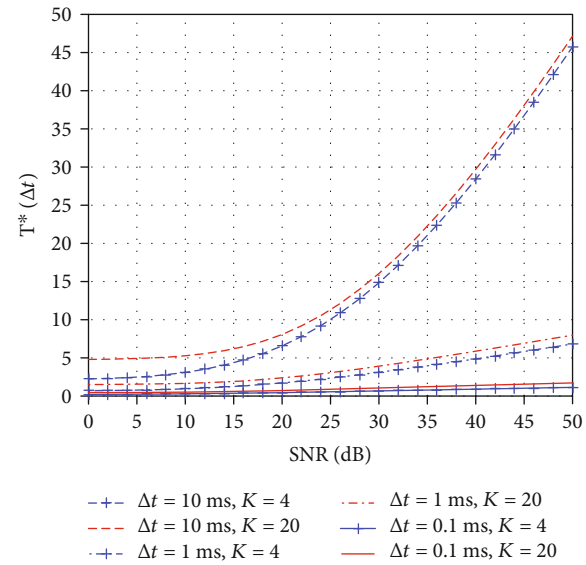

Figure 6: Optimal normalized T as a function of SNR

6.2. Maximum Rate Performance. This subsection investigates the behaviour of the deterministic maximum rate of OMC with different parameters. Firstly, we investigate how the maximum rate varies with communication time T. Assuming there are $K = 4$ users with an average speed of $v/K = 80$ Km/h, the curve of $\bar{R}_k$ (c.f. (13)) as a function of T is plotted in Figure 5 with different other parameters. It can be seen that $\bar{R}_k$ is indeed unimodal with respect to T. Again, Δt has important impact on the rate. The optimal T^* shrinks with decreased Δt, indicating the tendency of more concentrated power in this case. In addition, SNR also

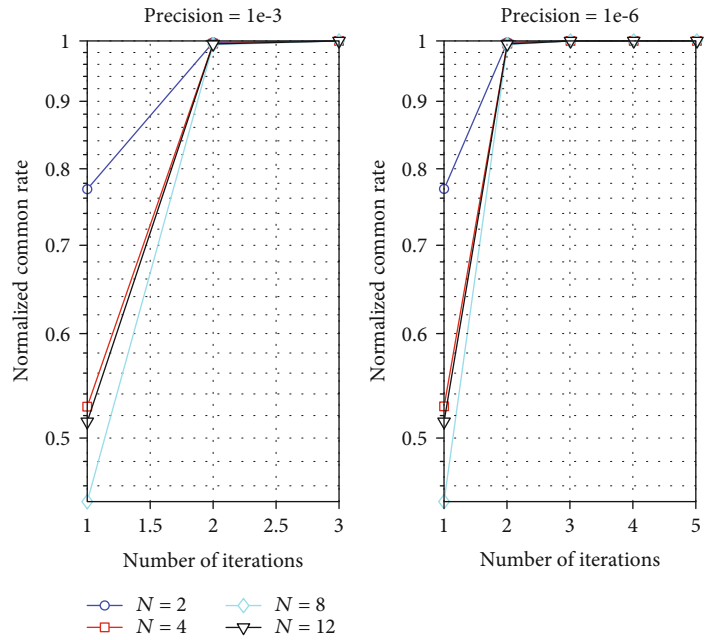

Figure 7: Convergence behaviour of the proposed user power allocation scheme with different rate precision

plays a key role here. To see it more clearly, Figure 6 shows how the optimal T, in the normalized form as $T^*/\Delta t$, changes with SNR. In general, a larger SNR results in a larger T^*. Finally, it is observed from Figure 6 that the number of users K does not have significant impact on the optimal T^*.

6.3. User Grouping and Power Allocation with Multiple SLMs. In this subsection, we simulate the performance of user grouping and power allocation with multiple SLMs. The speeds of users are set as uniformly distributed in the range of 70 ~ 120 Km/h. $\Delta t = 1$ ms switch time is assumed here.

Firstly, we show the convergence behaviour of the proposed user and group power allocation scheme described in Algorithm 1. Figure 7 shows how the rate converges with the number of iterations for different number of groups and numerical precisions. $K = 16$ is assumed here, and the precision is defined as the normalized ratio $(\mathscr{R}_{\max} - \mathscr{R}_{\min})/\mathscr{R}_{\max}$, where $\mathscr{R}_{\max}$ and $\mathscr{R}_{\min}$ denote the maximum and minimum per group rates (c.f. step 6 in Algorithm 1) in an iteration, respectively. The results are averaged over 500 random speed realizations. It can be seen from Figure 7 that the rate converges quickly with the number of iterations, indicating the effectiveness of the proposed power allocation algorithm.

Secondly, based on our proposed user grouping strategy, we show the potential gain of using multiple SLMs in power division usage mode, which is denoted by "OMC/PDU" in the legend, where "PDU" stands for power division usage. Figure 8 shows the maximum common rate with different system configurations. The results are also averaged over 500 random speed realizations. The number of users is fixed as $K = 16$, and $N = 2$ and 4 groups are tested. Several OMC schemes are compared here. For the proposed user grouping strategy, the results are labeled as "proposed UG" where

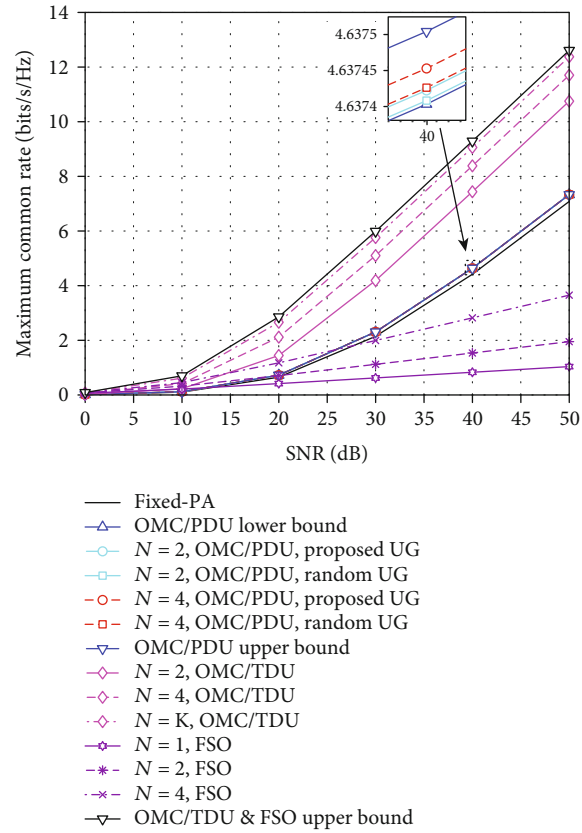

Figure 8: Maximum rate as a function of SNR for different schemes with multiple SLMs.

"UG" stands for user grouping. Similarly, the scheme with random user grouping is labeled as "random UG." When $N = 1$, there is no user grouping, and the results constitute a lower bound. When $N = K$, every user forms a single-

user group, and the result can be viewed as performance upper bound of power division usage mode. Power allocations in those schemes are all based on Algorithm 1. Performance of the fixed-PA scheme is also plotted here. Quite surprisingly, it can be seen from Figure 8 that although OMC is indeed superior to the fixed-PA scheme with noticeable gain, multiple SLMs with user grouping does not bring desirable performance gain, i.e., the lower bound and the upper bound are very close to each other. Nonetheless, by zoomed view, the gain of the proposed user grouping strategy over the random user grouping strategy can be still clearly observed, which validates the suboptimality analysis in Section 4. This seemingly discouraging result may be a good thing for engineering, as it suggests we only need a single SLM!

Beside the aforementioned schemes, the performance of time division usage of SLM discussed in Section 5 is also included in Figure 8 for comparison. All the curves obtained by this scheme is labeled by "OMC/TDU," where "TDU" stands for time division usage of multiple SLMs. Moreover, performance of the FSO scheme based on (28) is evaluated for comparison. Finally, the common upper bound of OMC/TDU and FSO is also plotted in the figure. It can be seen that with time division usage of multiple SLMs, the rate of OMC can be improved greatly compared with user grouping strategy with power division usage of SLMs. In addition, the rate increases with the number of SLMs and approaches to its upper bound. However, $N = 2$ can collect a fairly large portion of the benefit. Further increasing N brings only incremental gain. This confirms that $N = 2$ is a good complexity-performance tradeoff. On the other hand, for smaller N, OMC is also superior to the FSO scheme at high SNR region, which proves the effectiveness of the core idea of OMC, i.e., using SLMs to distribute power simultaneously.

7. Conclusions and Future Works

This paper investigated the rate performance of OMC system with user mobility through analysis and numerical examples. Due to the switch time of SLM, the communication must take place in periods separated by the minimum switch time. The optimal communication time and the corresponding rate were analyzed in this paper. It was found that mobility reduces the achievable rate in general. The rate loss can be compensated if the switch time of SLM can be reduced. Moreover, as OMC is capable of flexibly adjusting the power split ratios to generate a controllable channel, its rate performance is much better than the conventional scheme with fixed power split ratios. Then, two schemes integrating multiple SLMs, i.e., power division usage of multiple SLMs and time division usage of multiple SLMs, were studied in detail, respectively. It was found through simulations that power division usage of multiple SLMs brought little rate gain as compared to the single SLM case. On the other hand, time division usage of SLMs can compensate for the hardware deficiency of SLMs and boost the performance to a large extent. Compared with benchmark schemes, OMC is not only superior to the conventional scheme with fixed power allocation ratios but also outperforms FSO at high SNR regime.

Following this work and the above conclusions, there are many new issues that are worth studying in the future. For instance, even advanced SLM with reduced switch time is used in the future, the communication time T can still not be very small; otherwise, the localization precision requirement would be very stringent. A practical approach with lower costs is to use intensity modulation, which would have very different signal models and derivations. Another research point is to study the unicast communication scenario with user mobility and multiple light sources, which is more attractive for future applications and more challenging. In addition, integration with uplink transmission can be an important topic from a system point of view. Demonstration of prototype would be of key importance to evaluate how far this new technology can go.

Appendix

A. Proof of Proposition 1

$$\tilde{R}_k(T, v_k) = \bar{R}_k(1, T, v_k) = \frac{T}{T + \Delta t} \log_2\left(1 + \frac{D\gamma}{v_k T + D}\right). \tag{A.1}$$

To prove $\tilde{R}_k(T, v_k)$ is unimodal with respect to T, it is sufficient to show $(\partial \tilde{R}_k(T, v_k))/\partial T$ has only a single root in $(0, \infty)$, since $\tilde{R}_k(T, v_k) > 0$ and $\lim_{T \longrightarrow 0} \tilde{R}_k(T, v_k) = \lim_{T \longrightarrow \infty} \tilde{R}_k(T, v_k) = 0$. Set $(\partial \tilde{R}_k(T, v_k))/\partial T = 0$ and simplify it, we can obtain

$$\frac{\Delta t}{T + \Delta t} \ln\left(1 + \frac{D\gamma}{v_k T + D}\right) = \frac{D\gamma v_k T}{[v_k T + D(\gamma + 1)](v_k T + D)}. \tag{A.2}$$

Define $b_k = v_k \Delta t$ and $s_k = D\gamma/(v_k T + D)$, then $s_k \in (0, \gamma)$ and (A.2) can be reformulated as

$$\gamma b_k (1 + s_k) \ln(1 + s_k) + (b_k - D)s_k^2 + \gamma(2D - b_k)s_k - D\gamma^2 = 0. \tag{A.3}$$

Denoting $h(s_k)$ as the left-hand side of (A.3), the original problem is equivalent to show that $h(s_k)$ has only a single root on $s_k \in (0, \gamma)$. As $\lim_{s_k \longrightarrow 0} h(s_k) < 0$ and $\lim_{s_k \longrightarrow \gamma} h(s_k) > 0$, we can conclude that $h(s_k)$ has at least one root. The first-order derivative of $h(s_k)$ is given by

$$h'(s_k ; b_k) = \gamma b_k \ln(1 + s_k) + 2(b_k - D)s_k + 2D\gamma, \tag{A.4}$$

which is an increasing function of b_k for any fixed s_k. In particular, $h'(s_k ; 0) = 2D(\gamma - s_k) > 0$ for $s_k \in (0, \gamma)$. Therefore, $h'(s_k ; b_k) > 0$ in its domain of definition with respect to s_k, for any given $b_k \geq 0$. This means $h(s_k)$ is a monotonically increasing function of s_k. Therefore, $h(s_k)$ has and

only has one root over $s_k \in (0, \gamma)$, which finally leads to the conclusion that $\tilde{R}_k(T, v_k)$ is unimodal.

B. Proof of Proposition 4

We first investigate a special case where $N = 2$ to reveal the behaviour of proposed user grouping strategy. According to Section 3.3, for any user group, the maximum rate is related to the number of users in this group and the summation of their speeds. We rewrite (17) by

$$\mathscr{R}_i(T_i, \beta_i, \Delta_v) = \frac{T_i}{T_i + \Delta t} \log_2\left(1 + \frac{\beta_i D\gamma}{((v/2) + \Delta_v)T_i + k_i D}\right), \tag{B.1}$$

where $k_n = |\mathscr{K}_n|$, v is the sum speed of all the K users, $((v/2) - \Delta_v)$ and $((v/2) + \Delta_v)$, with $0 < \Delta_v \le (v/2)$, denote the sum speeds of the two groups after user grouping, respectively. The maximum common rate of the two groups is given by

$$\mathscr{R}(\Delta_v) = \max_{\{T_1, T_2, \beta_1, \beta_2\}} \mathscr{R}_1(T_1, \beta_1, \Delta_v), \tag{B.2}$$

with constraints $\beta_1 + \beta_2 = 1$ and $\mathscr{R}_1(T_1, \beta_1, \Delta_v) = \mathscr{R}_2(T_2, \beta_2, \Delta_v)$. By treating Δ_v as a continuous variable, we have the following lemma.

Lemma B.1. *For given Δt, D, $v > 0$, $\gamma > 0$, and $k_n > 0$, $n = 1, 2$, $\mathscr{R}(\Delta_v)$ is an increasing function of Δ_v for $0 < \Delta_v \le v/2$ at low SNR regime.*

Proof of Lemma B.1. For notational simplicity, we replace the base-2 logarithmic function by the natural logarithmic function and take the following variable changes: $t_n \triangleq (T_n/\Delta t)$, $\tilde{v} \triangleq (v\Delta_t/2D\gamma)$, $\tilde{k}_n = (k_n/\gamma)$, $\tilde{\Delta}_v = (\Delta_v\Delta_t/D\gamma)$, where $0 < \tilde{\Delta}_v \le \tilde{v}$. The rate pairs in (B.1) can be reformulated as

$$\mathscr{R}_i\left(t_i, \beta_i, \tilde{\Delta}_v\right) = \frac{t_i}{t_i + 1} \ln\left(1 + \frac{\beta_i}{\left(\tilde{v} + \tilde{\Delta}_v\right)t_i + \tilde{k}_i}\right). \tag{B.3}$$

□

The optimization variables are t_i and β_i, $i = 1, 2$. The known quantities are $\tilde{v}$, $\tilde{\Delta}_v$, $\tilde{k}_1$, and $\tilde{k}_2$. When γ is very small, the rates can be approximated as

$$\mathscr{R}_i\left(t_i, \beta_i, \tilde{\Delta}_v\right) \approx \frac{t_i}{t_i + 1} \frac{\beta_i}{\left(\tilde{v} + \tilde{\Delta}_v\right)t_i + \tilde{k}_i}. \tag{B.4}$$

It can be shown that the maximum values of the rates are given by

$$\mathscr{R}_i^*\left(\beta_i, \tilde{\Delta}_v\right) = \frac{\beta_i}{\left(\sqrt{\tilde{v} + \tilde{\Delta}_v} + \sqrt{\tilde{k}_i}\right)^2}, \tag{B.5}$$

which are achieved at $t_1^* = \sqrt{(\tilde{k}_1/(\tilde{v} - \tilde{\Delta}_v))}$ and $t_2^* = \sqrt{(\tilde{k}_2/(\tilde{v} - \tilde{\Delta}_v))}$, respectively. The maximum common rate of the two user groups is given by

$$\mathscr{R}\left(\tilde{\Delta}_v\right) = \max_{\{\beta_1\}} \mathscr{R}_1^*\left(\beta_1, \tilde{\Delta}_v\right), \tag{B.6}$$

with constraints of $\mathscr{R}_1^*(\beta_1, \tilde{\Delta}_v) = \mathscr{R}_2^*(\beta_2, \tilde{\Delta}_v)$ and $\beta_1 + \beta_2 = 1$. The solution of problem (B.6) can be readily obtained as

$$\mathscr{R}\left(\tilde{\Delta}_v\right) = \frac{1}{\left(\sqrt{\tilde{v} - \tilde{\Delta}_v} + \sqrt{\tilde{k}_1}\right)^2 + \left(\sqrt{\tilde{v} + \tilde{\Delta}_v} + \sqrt{\tilde{k}_2}\right)^2}, \tag{B.7}$$

which is an increasing function of $\tilde{\Delta}_v$ for $0 < \tilde{\Delta}_v \le \tilde{v}$. This in turn proves Lemma B.1.

Now, we consider optimality only in the low SNR regime. When $N = 2$, Lemma B.1 immediately leads to Proposition 4 since $(v/2) - v_1$ is the maximum feasible value of Δ_v for given speed sets. When $N > 2$, we consider any other potential optimal user grouping strategy given by $\mathscr{K}'_n$, $n = 1, 2, \cdots, N$, excluding the trivial cases in which $\{\mathscr{K}'_n\}_{n=1}^N$ is just a permutation of $\{\mathscr{K}_n\}_{n=1}^K$. In $\{\mathscr{K}'_n\}_{n=1}^N$, there must exist at least one such user group that this group consists of more than one user, and at the same time, this group contains at least one of the users with indices $1, 2, \cdots, N-1$. Otherwise, the grouping strategy is the same with $\{\mathscr{K}_n\}_{n=1}^K$. Locating a specific user m, $m \in \{1, 2, \cdots, N-1\}$, such that user m is in a user group, denoted by $\mathscr{K}'_{\tilde{m}}$ which had more than one user, but for any l, $l < m$, user l forms a single-user group. As $m < N$, there is at least one other group, denoted by $\mathscr{K}'_{\tilde{m}+1}$, that does not contain users $1, 2, \cdots, m$. If we regroup the users in $\mathscr{K}'_{\tilde{m}}$ and $\mathscr{K}'_{\tilde{m}+1}$, according to Lemma B.1, the optimal strategy is to isolate user m in a single-user group, and all the other users form the other group, as v_m is the lowest speed. This is in contradiction with the preassumption that the grouping is already optimal. Therefore, Proposition 4 is proved.

Data Availability

The data is available from the corresponding author upon request.

Disclosure

Part of this paper was published in the proceeding of 2019 IEEE Global Communications Conference.

Conflicts of Interest

The authors declare that there is no conflict of interest regarding the publication of this paper.

Acknowledgments

This work was supported by the National Key R&D Program of China under grants 2018YFB1801101 and 2016YFB0502202, NSFC projects (61971136, 61960206005, and 61803211), NSF of Jiangsu Province project (No. BK20191261), Zhejiang Lab (No. 2019LC0AB02), the Fundamental Research Funds for the Central Universities, Young Elite Scientist Sponsorship Program by CAST (YESS20160042), and Zhishan Youth Scholar Program of SEU.

References

[1] M. Shafi, A. F. Molisch, P. J. Smith et al., "5G: a tutorial overview of standards, trials, challenges, deployment, and practice," *IEEE Journal on Selected Areas in Communications*, vol. 35, no. 6, pp. 1201–1221, 2017.

[2] T. S. Rappaport, S. Sun, R. Mayzus et al., "Millimeter wave mobile communications for 5G cellular: it will work!," *IEEE Access*, vol. 1, pp. 335–349, 2013.

[3] M. Giordani, M. Polese, A. Roy, D. Castor, and M. Zorzi, "A tutorial on beam management for 3GPP NR at mmWave frequencies," *IEEE Communications Surveys & Tutorials*, vol. 21, no. 1, pp. 173–196, 2019.

[4] E. G. Larsson, O. Edfors, F. Tufvesson, and T. L. Marzetta, "Massive MIMO for next generation wireless systems," *IEEE Communications Magazine*, vol. 52, no. 2, pp. 186–195, 2014.

[5] J. G. Andrews, H. Claussen, M. Dohler, S. Rangan, and M. C. Reed, "Femtocells: past, present, and future," *IEEE Journal on Selected Areas in Communications*, vol. 30, no. 3, pp. 497–508, 2012.

[6] D. J. C. MacKay, "Good error-correcting codes based on very sparse matrices," *IEEE Transactions on Information Theory*, vol. 45, no. 2, pp. 399–431, 1999.

[7] E. Arikan, "Channel polarization: a method for constructing capacity-achieving codes for symmetric binary-input memoryless channels," *IEEE Transactions on Information Theory*, vol. 55, no. 7, pp. 3051–3073, 2009.

[8] H. Nikopour and H. Baligh, "Sparse code multiple access," in *2013 IEEE 24th Annual International Symposium on Personal, Indoor, and Mobile Radio Communications (PIMRC)*, pp. 332–336, London, UK, September 2013.

[9] L. Dai, B. Wang, Z. Ding, Z. Wang, S. Chen, and L. Hanzo, "A survey of non-orthogonal multiple access for 5G," *IEEE Communications Surveys & Tutorials*, vol. 20, no. 3, pp. 2294–2323, 2018.

[10] X. You, C. X. Wang, J. Huang et al., "Towards 6G wireless communication networks: vision, enabling technologies, and new paradigm shifts," *SCIENCE CHINA Information Sciences*, vol. 64, no. 1, pp. 1–74, 2021.

[11] K. David and H. Berndt, "6G vision and requirements: is there any need for beyond 5G?," *IEEE Vehicular Technology Magazine*, vol. 13, no. 3, pp. 72–80, 2018.

[12] T. S. Rappaport, Y. Xing, O. Kanhere et al., "Wireless communications and applications above 100 GHz: opportunities and challenges for 6G and beyond," *IEEE Access*, vol. 7, pp. 78729–78757, 2019.

[13] Y. Zhao, G. Yu, and H. Xu, "6G mobile communication networks: vision, challenges, and key technologies," *SCIENTIA SINICA Informationis*, vol. 49, no. 8, pp. 963–987, 2019.

[14] Z. Zhang, L. Wu, J. Dang et al., "Optical mobile communications: principles and challenges," in *2017 26th Wireless and Optical Communication Conference (WOCC)*, Newark, USA, April 2017.

[15] H. Zhang, Z. Ji, H. Wang, and W. Wu, "Survey on quantum information security," *China Communications*, vol. 16, no. 10, pp. 1–36, 2019.

[16] L. E. M. Matheus, A. B. Vieira, L. F. M. Vieira, M. A. M. Vieira, and O. Gnawali, "Visible light communication: concepts, applications and challenges," *IEEE Communications Surveys & Tutorials*, vol. 21, no. 4, pp. 3204–3237, 2019.

[17] P. W. Berenguer, P. Hellwig, D. Schulz et al., "Real-time optical wireless mobile communication with high physical layer reliability," *Journal of Lightwave Technology*, vol. 37, no. 6, pp. 1638–1646, 2019.

[18] H. B. Eldeeb, S. M. Mana, V. Jungnickel, P. Hellwig, J. Hilt, and M. Uysal, "Distributed MIMO for Li-Fi: channel measurements, ray tracing and throughput analysis," *IEEE Photonics Technology Letters*, vol. 33, no. 16, pp. 916–919, 2021.

[19] Z. Zhang, J. Dang, L. Wu et al., "Optical mobile communications: principles, implementation, and performance analysis," *IEEE Transactions on Vehicular Technology*, vol. 68, no. 1, pp. 471–482, 2019.

[20] J. Dang, J. Gao, Z. Zhang, L. Wu, and B. Zhu, "On the achievable rate performance of broadcast OMC system with user mobility," in *2019 IEEE Globecom Workshops (GC Wkshps)*, Hawaii, USA, December 2019.

[21] J. Gao, J. Dang, Z. Zhang, and L. Wu, "Rate analysis of intensity modulated broadcast optical mobile communication system with user mobility," *IEEE Photonics Journal*, vol. 12, no. 5, pp. 1–12, 2020.

[22] A. Belmonte and J. M. Kahn, "Field conjugation adaptive arrays in free-space coherent laser communications," *Journal of Optical Communications and Networking*, vol. 3, no. 11, pp. 830–838, 2011.

[23] S. Bae, J. Park, S. Kim, and G. Yoon, "Performance analysis of coherent FSO-OFDM systems with frequency offset," *IEEE Communications Letters*, vol. 20, no. 11, pp. 2189–2192, 2016.

[24] Y. Tu, S. Cui, K. Zhou, and D. Liu, "Phase alignment with minimum complexity for equal gain combining in multi-aperture free-space digital coherent optical communication receivers," *IEEE Photonics Journal*, vol. 12, no. 2, article 7901410, 2020.

[25] C. Yue, J. Li, J. Sun et al., "Homodyne coherent optical receiver for intersatellite communication," *Applied Optics*, vol. 57, no. 27, pp. 7915–7923, 2018.

[26] S. Aboagye, T. M. N. Ngatched, O. A. Dobre, and A. Ibrahim, "Joint access point assignment and power allocation in multitier hybrid RF/VLC HetNets," *IEEE Transactions on Wireless Communications*, pp. 1–1, 2021.

[27] H. B. Eldeeb, M. Hosney, H. M. Elsayed, R. I. Badr, M. Uysal, and H. A. I. Selmy, "Optimal resource allocation and interference management for multi-user uplink light communication systems with angular diversity technology," *IEEE Access*, vol. 8, pp. 203224–203236, 2020.

[28] S. Ma, F. Zhang, H. Li, F. Zhou, M. S. Alouini, and S. Li, "Aggregated VLC-RF systems: achievable rates, optimal power allocation, and energy efficiency," *IEEE Transactions on Wireless Communications*, vol. 19, no. 11, pp. 7265–7278, 2020.

[29] J. Hu, Z. Zhang, J. Dang, L. Wu, and G. Zhu, "Investigation of a coherent optical wireless system for high speed indoor

interconnection," *Optics Communications*, vol. 438, pp. 111–117, 2019.

[30] K. Zhang, B. Zhu, Z. Zhang, and H. Wang, "Tracking system for optical mobile communication and the design rules," *IEEE Transactions on Wireless Communications*, vol. 20, no. 4, pp. 2716–2728, 2021.

[31] K. Kikuchi and S. Tsukamoto, "Evaluation of sensitivity of the digital coherent receiver," *Journal of Lightwave Technology*, vol. 26, no. 13, pp. 1817–1822, 2008.

[32] A. Prokeš, "Modeling of atmospheric turbulence effect on terrestrial FSO link," *Radioengineering*, vol. 18, no. 1, pp. 42–47, 2009.

[33] A. A. Farid and S. Hranilovic, "Outage capacity optimization for free-space optical links with pointing errors," *Journal of Lightwave Technology*, vol. 25, no. 7, pp. 1702–1710, 2007.

[34] C. E. Shannon, "A mathematical theory of communication," *The Bell System Technical Journal*, vol. 27, no. 3, 1948.

[35] B. C. Rennie and A. J. Dobson, "On stirling numbers of the second kind," *Journal of Combinatorial Theory*, vol. 7, no. 2, pp. 116–121, 1969.